

PHYSICAL REVIEW LETTERS

VOLUME 40

2 JANUARY 1978

NUMBER 1

Clean Tests of Quantum Chromodynamics in μp Scattering

Howard Georgi

Lyman Laboratory of Physics, Harvard University, Cambridge, Massachusetts 02138

and

H. David Politzer

California Institute of Technology, Pasadena, California 91125

(Received 25 October 1977)

Hard gluon bremsstrahlung in μp scattering produces final-state hadrons with a large component of momentum transverse to the virtual-photon direction. Quantum chromodynamics can be used to predict not only the absolute value of the transverse momentum, but also its angular distribution relative to the muon scattering plane. The angular correlations should be insensitive to nonperturbative effects.

In this Letter we report selected results from a study of semi-inclusive μp scattering. Our analysis is based on QCD (quantum chromodynamics) perturbation theory¹ and the parton-model idea of decay functions.² Let k_1 (k_2) be the initial (final) muon four-momentum and P_1 (P_2) be the target (observed final-state hadron) four-momentum. At high energy, the hadrons will be produced in a jet with momenta nearly parallel to the virtual-photon direction, $q^\mu = k_1^\mu - k_2^\mu$. Some of our most interesting results involve the transverse momentum $\vec{P}_{2\perp}$, perpendicular to \vec{q} .

Integrating over the azimuthal angle of the final muon, we can write the differential cross section in terms of the variables

$$Q^2 = -q^2, \quad x_H = Q^2/2P_1 \cdot q, \quad y = P_1 \cdot q / P_1 \cdot k_1, \quad z_H = P_1 \cdot P_2 / P_1 \cdot q, \quad P^2 = |\vec{P}_{2\perp}|^2, \quad \text{and } \varphi, \quad (1)$$

where φ is the azimuthal angle of $\vec{P}_{2\perp}$ measured from $\vec{k}_{1\perp}$, the component of the initial μ momentum orthogonal to \vec{q} .

The underlying assumption in the analysis is that the semi-inclusive cross section can be written as an integral over parton variables as follows:

$$\frac{d\sigma}{dx_H dy dz_H dP_{1\perp}^2 d\varphi} \simeq \sum_{j,k} dx_p dz_p dp_{1\perp}^2 d\xi d\xi' \delta(x_H - \xi x_p) \delta(z_H - \xi' z_p) \delta(P_{1\perp}^2 - \xi'^2 p_{1\perp}^2) \times f_j(\xi, Q^2) \frac{d\sigma_{jk}}{dx_p dy dz_p dp_{1\perp}^2 d\varphi} d_k(\xi', Q^2). \quad (2)$$

The sum over j and k runs over all partons (quarks, antiquarks, and gluons). The cross section $d\sigma_{jk}$ describes the semi-inclusive process

$\mu(k_1) + j \text{ parton}(p_1) \rightarrow \mu(k_2) + k \text{ parton}(p_2) + \text{anything.}$

The parton scaling variables are defined by

$$x_p = Q^2/2p_1 \cdot q, \quad z_p = p_1 \cdot p_2/p_1 \cdot q. \quad (3)$$

f_j and d_k are parton distribution and decay functions, suitably corrected to include certain interaction effects; $f_j(\xi, Q^2)$ describes the probability distribution for j partons with a fraction ξ of the target momentum, $p_1 = \xi P_1$; $d_k(\xi', Q^2)$ describes the probability distribution for a k parton to decay into a hadron with a fraction ξ' of the parton momentum, $P_2 = \xi' p_2$.

The point of Eq. (2) is that $d\sigma_{jk}$ and the Q^2 dependence of f_j and d_k can be calculated with use of perturbation theory. We assume that the large logarithms (and/or infrared divergences) which occur in perturbation theory factorize and can be associated with the f and d functions whose overall shape must be taken from experiment. In Eq. (2), the factorization has already been implemented. Terms of order p_\perp^2/Q^2 have been ignored and all dependence on $\ln(p_\perp^2/Q^2)$ [$\ln(p_2^2/Q^2)$] has been absorbed into the distribution [decay] function $f_j(\xi, Q^2)$ [$d_k(\xi', Q^2)$]. The analogous assumption in totally inclusive μp scattering is proven by use of the operator product expansion. No proof exists for the semi-inclusive process, but we have checked that the required factorization takes place to lowest nontrivial order in α_s . These details will be presented elsewhere.

In zeroth order in α_s , the parton cross section is pointlike:

$$\frac{d\sigma_{jk}}{dx_p dy dz_p dP_\perp^2 d\varphi} = \frac{\alpha^2}{y Q^2} [1 + (1-y)^2] Q_j^2 \delta_{jk} \delta(1-x_p) \delta(1-z_p) \delta(P_\perp^2), \quad (4)$$

where Q_j is the parton (quark) charge. Inserted into Eq. (2), this gives the standard parton-model result,

$$\frac{d\sigma}{dx_H dy dz_H dP_\perp^2 d\varphi} = \frac{\alpha^2}{y Q^2} [1 + (1-y)^2] \sum_j Q_j^2 f_j(x_H) d_j(z_H) \delta(P_\perp^2). \quad (5)$$

Some of the most interesting results of the perturbative analysis concern features which are totally absent in zeroth order, such as nonzero P_\perp and nontrivial φ dependence.

As an illustration of the power of the perturbative technique, we quote the results for the expectation value of $\cos\varphi$, which measures the front-to-back asymmetry of $\vec{P}_{2\perp}$ along the $\vec{k}_{1\perp}$ direction. We first compute the integral of $\cos\varphi$ in the diagrams depicted in Fig. 1. The result is the following formidable expression:

$$\int \cos\varphi d\varphi dP_\perp^2 \frac{d\sigma}{dx_H dy dz_H dP_\perp^2 d\varphi} = \frac{2\pi\alpha^2 4}{y Q^2 3} \frac{\alpha_s}{\pi} \int_{x_H}^1 \frac{dx_p}{x_p} \int_{z_H}^1 \frac{dz_p}{z_p} (2-y)(1-y)^{1/2} \sum_j Q_j^2 [A_j + B_j + C_j], \quad (6)$$

where A , B , and C arise from the diagrams in Figs. 1(a)–1(c), respectively. The individual contributions are

$$A_j = -f_j\left(\frac{x_H}{x_p}, Q^2\right) [x_p z_p + (1-x_p)(1-z_p)] \left(\frac{x_p z_p}{(1-x_p)(1-z_p)}\right)^{1/2} d_j\left(\frac{z_H}{z_p}, Q^2\right), \quad (7a)$$

$$B_j = f_j\left(\frac{x_H}{x_p}, Q^2\right) [x_p(1-z_p) + (1-x_p)z_p] \left(\frac{x_p(1-z_p)}{(1-x_p)z_p}\right)^{1/2} d_G\left(\frac{z_H}{z_p}, Q^2\right), \quad (7b)$$

$$C_j = \frac{3}{8} f_G\left(\frac{x_H}{x_p}, Q^2\right) (1-2z_p)(1-2x_p) \left(\frac{x_p(1-x_p)}{z_p(1-z_p)}\right)^{1/2} d_j\left(\frac{z_H}{z_p}, Q^2\right), \quad (7c)$$

where j labels the quark or antiquark coupled to the electromagnetic current, and G labels a gluon distribution or decay function.

Evidently, the scattered quark in Fig. 1(a) is produced with p_\perp opposite to k_\perp [A_j is negative, Eq. (7a)]. Of course, the gluon is produced with the opposite p_\perp . In fact, the gluon contribution is given by Eq. (7b), obtained from Eq. (7a) by the replacement $z_p \rightarrow 1-z_p$ and changing the sign. At small z_H ,

both A and B contribute and the sign of $\langle \cos\phi \rangle$ depends on the detailed comparison of quark- and gluon-decay functions. However, at large z_H (and therefore large z_H/z_p), it is reasonable to assume that the gluon-decay function (into pions for example) is small compared to the quark-decay function. If that is the case $A_j \gg B_j$ at large z_H , and struck quarks tend to produce hadrons with negative $\langle \cos\phi \rangle$.

The contribution from gluons in the target [Eq. (7c)] can have either sign. But at small x_H , another simplification occurs. If $f_G(\xi) \rightarrow k/\xi$ as $\xi \rightarrow 0$, the contribution of Eq. (7c) integrates to zero as $x_H \rightarrow 0$ (the quark-antiquark pair is produced symmetrically). Furthermore, if $f_j(\xi) \rightarrow k_j/\xi$ as $\xi \rightarrow 0$, the quark contributions do not depend on the shape of the distribution functions, but only on k_j . As $x_H \rightarrow 0$ for large z_H , we can write a simple expression for $\langle \cos\phi \rangle$, to first order in α_s ,

$$\langle \cos\phi \rangle \simeq -\frac{4}{3} \frac{\alpha_s}{\pi} \frac{(2-y)(1-y)^{1/2}}{[1+(1-y)^2]D(z_H, Q^2)} \int_{z_H}^1 \frac{dz_p}{z_p} D\left(\frac{z_H}{z_p}, Q^2\right) \frac{\pi}{8} \left\{ 3 \frac{z_p^{3/2}}{(1-z_p)^{1/2}} + [z_p(1-z_p)]^{1/2} \right\}, \quad (8)$$

where

$$D(\xi, Q^2) = \sum_j Q_j^2 k_j d_j(\xi, Q^2). \quad (9)$$

The effective decay function $D(\xi, Q^2)$ is directly measured in the semi-inclusive cross section at small x_H , which is

$$\frac{d\sigma}{dx_H dy dz_H} = \frac{4\pi \alpha^2 m E}{Q^4} D(z_H, Q^2) \quad (10)$$

to lowest order in α_s as $x_H \rightarrow 0$.

Equation (8) should be valid for any z_H at which the gluon-decay function is negligible compared to the quark-decay functions. As $z_H \rightarrow 1$, we can simplify still further to

$$\langle \cos\phi \rangle = -\frac{\pi}{2} \frac{\alpha_s}{\pi} \frac{(2-y)(1-y)^{1/2}}{[1+(1-y)^2]} \kappa (1-z_H)^{1/2} + O((1-z_H)^{3/2}), \quad (11)$$

where

$$\kappa = \lim_{z_H \rightarrow 1} \left\{ \int_{z_H}^1 dz (1-z)^{-1/2} D(z_H/z, Q^2) [(1-z_H)^{1/2} D(z_H, Q^2)]^{-1} \right\}. \quad (12)$$

The constant κ depends only weakly on the shape of $D(\xi, Q^2)$: $\kappa \simeq 1$ if $D(\xi, Q^2) \propto (1-\xi)^3$ for large ξ .

Other predictions of QCD for semi-inclusive μp scattering, along with a demonstration of factorization of the parton cross section to first order in α_s , will be given in a forthcoming paper. Meanwhile, there are two nice features of the predictions of Eqs. (6), (8), and (11) which demand attention. Firstly, the predicted asymmetries are rather large. For example, with initial μ energy of 200 GeV, $x_H = 0.05$, $y = 0.3$, and $z_H = 0.7$, Eq. (11) (with $\kappa \simeq 1$) gives $\langle \cos\phi \rangle \simeq -0.12$ corresponding to a back-to-front asymmetry of 15%. Effects this large should be detectable even though data at high z_H are scarce. Secondly, the nonperturbative effects of quark confinement should not produce this kind of asymmetric ϕ distribution at $x_H \simeq 0$. Measurements of $\langle \cos\phi \rangle$ will provide a very clean test of the perturbative predictions of QCD.

One of us (H.G.) wishes to thank A. L. Sessoms for several useful conversations. This research was supported in part by the Alfred P. Sloan Foundation, the National Science Foundation un-

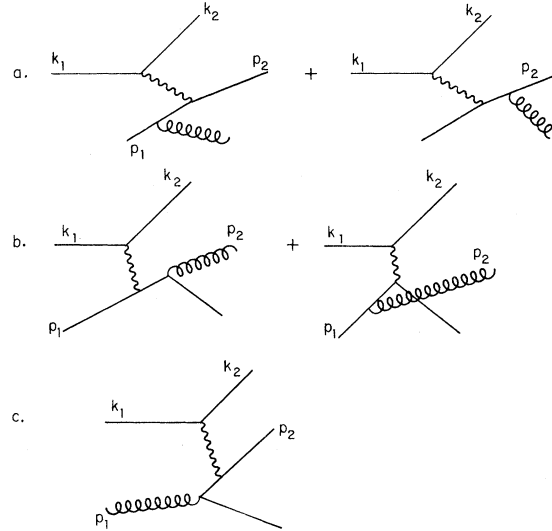


FIG. 1. Diagrams contributing to semi-inclusive μ -parton scattering to first order in α_s . k (p) denotes muon (parton) momentum. The wavy line is a virtual photon. The curly line is a gluon.

der Grant No. PHY75-20427, and the U. S. Energy Research and Development Administration under Contract No. EY76-C-03-0068.

¹See, for example, H. D. Politzer, Phys. Rep. **14C**, 129 (1974).

²See, for example, A. Mueller, Phys. Rev. D **9**, 963 (1974).

Comparison of $K^\pm N$ Charge-Exchange Reactions at 8.5 and 13 GeV/c

M. G. D. Gilchriese,^(a) W. Dunwoodie, T. Fieguth, D. P. Hutchinson, W. B. Johnson, P. F. Kunz, T. A. Lasinski, D. W. G. S. Leith, W. T. Meyer, B. N. Ratcliff, P. Schacht,^(b) S. Shapiro, and S. H. Williams

Stanford Linear Accelerator Center, Stanford University, Stanford, California 94305

and

M. Marshall and J. Scheid

California Institute of Technology, Pasadena, California 91109

and

C.-Y. Chien, L. Madansky, A. Pevsner, C. Woody, and R. A. Zdanis

Johns Hopkins University, Baltimore, Maryland 21218

(Received 2 August 1977)

The cross sections for the line-reversed reaction pairs $K^+n \rightarrow K^0p$ and $K^-p \rightarrow \bar{K}^0n$, and $K^+p \rightarrow K^0\Delta^{++}$ and $K^-n \rightarrow \bar{K}^0\Delta^-$ have been determined with high statistics and good relative normalization at 8.36 and 12.8 GeV/c in a spectrometer experiment at Stanford Linear Accelerator Center. The cross sections for the K^+ -induced reactions are larger than for the K^- , contrary to the expectations of weakly-exchange-degenerate Regge-pole models. The ratio of the reaction cross sections is about the same as at lower energies and shows little change with momentum transfer.

The dominant t -channel exchanges for the reactions,

$$K^+n \rightarrow K^0p, \quad (1a)$$

$$K^-p \rightarrow \bar{K}^0n, \quad (1b)$$

are the ρ and A_2 trajectories. Simple weakly-exchange-degenerate Regge-pole models¹ predict that the cross sections for these two reactions should be equal. Previous detailed comparisons of (1a) and (1b) have determined that the ratio of the K^+ to K^- total cross section is essentially constant from 3 to 6 GeV/c at a value of about 1.3.^{2,3}

The situation for the reactions,

$$K^+p \rightarrow K^0\Delta^{++}(1236), \quad (2a)$$

$$K^-n \rightarrow \bar{K}^0\Delta^-(1236), \quad (2b)$$

is similar; the cross-section ratio for this pair has been observed at 4 and 6 GeV/c and is greater than for Reactions (1).³

This Letter describes a comparison of the reactions pairs (1) and (2) at 8.36 and 12.8 GeV/c with high statistics and good relative normalization. The experiment was performed using the

downstream spectrometer of the large-aperture solenoid spectrometer (LASS) at Stanford Linear Accelerator Center.⁴ An rf-separated kaon beam was incident upon a 90-cm-long liquid deuterium target. The production of a K^0 was detected via the $K_s^0 \rightarrow \pi^+\pi^-$ decay mode using the wire spark chambers and scintillation-counter hodoscopes in the spectrometer.

Reactions (1) and (2) were identified by means of the distribution in the square of the missing mass (M_x^2) recoiling against the K^0 . The K^0 sample was defined by assuming the particles to be pions and then requiring the two-particle effective mass to be in the interval 0.478–0.518 GeV [Fig. 1(a)]. The M_x^2 calculated for these events is shown for the 8.36-GeV/c K^+ data in Fig. 1(b), the distributions for the other charge and energy being similar except for poorer resolution at the higher energy. Fermi motion did not significantly affect the M_x^2 resolution for the momentum-transfer region being studied.

The number of events for the reactions of interest was obtained by fitting a four-component function to the M_x^2 distribution for each $t' = t - t_{\min}$ interval, where t is the four-momentum transfer